

Gigahertz-peaked spectra pulsars

Karolina Rożko

in collaboration with

Wojciech Lewandowski, Jarosław Kijak, Rahul Basu

The University of Zielona Góra

Janusz Gil Institute of Astronomy, Poland

May 11, 2021

(Radio) Pulsars and their spectra

Rapidly rotating highly magnetised neutron stars

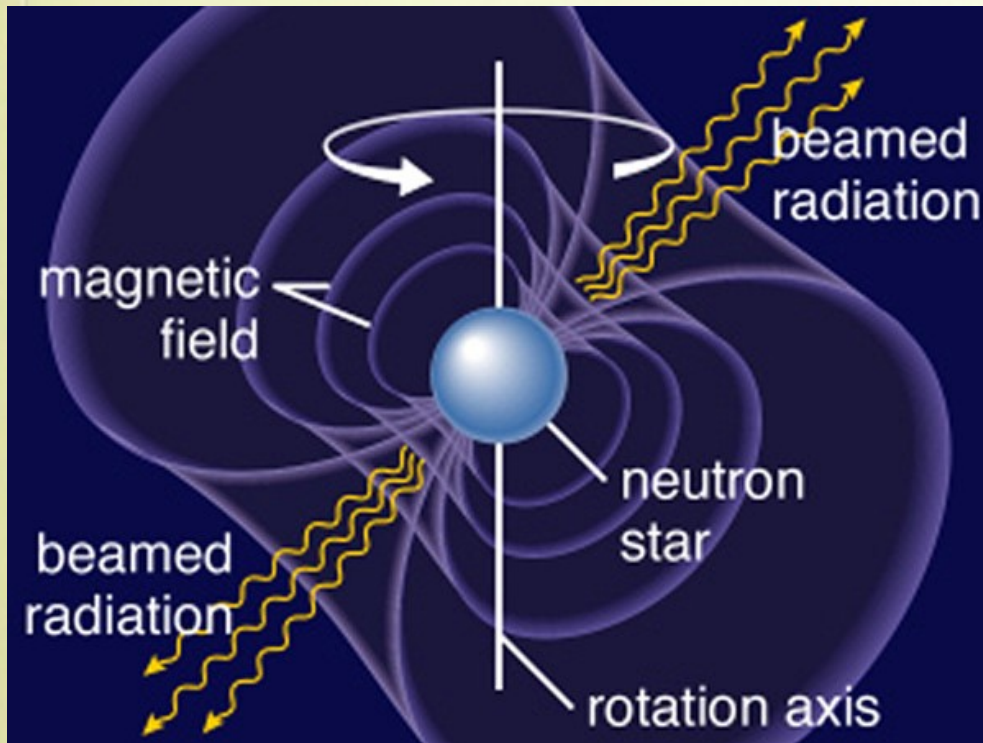


Figure 1: The model of the pulsar magnetosphere.

Picture from: <http://astronomy.nmsu.edu>.

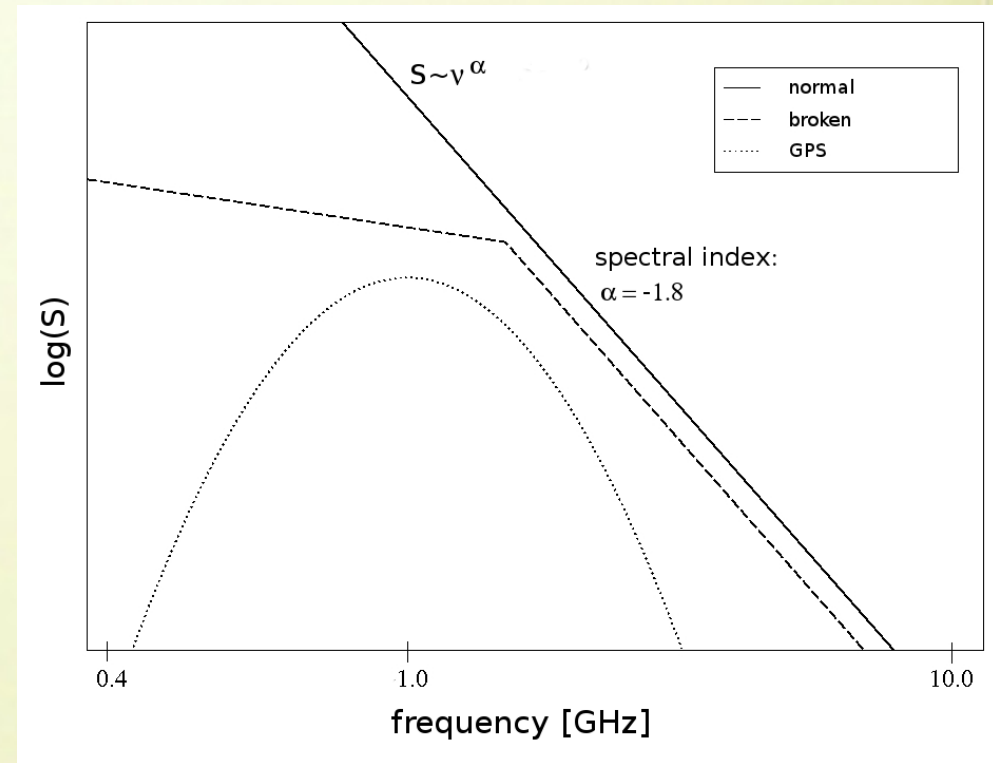


Figure 2: The morphological classification of the pulsar's radio spectra in the frequency range 100 MHz – 10 GHz.

A case of B1259-63 + Be star

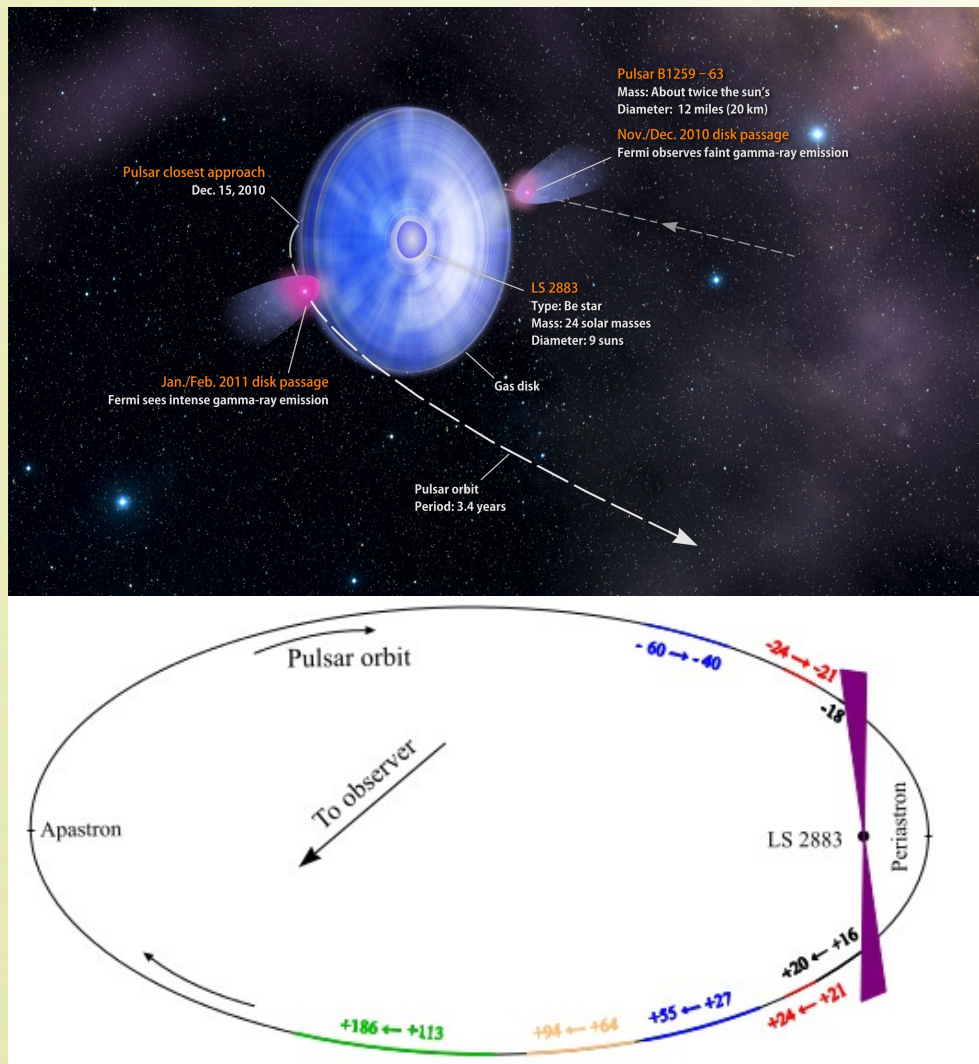


Figure 3: Top: The view of a binary pulsar B1259-63 with Be star LS 2883 from Earth (image credit: www.nasa.gov). Bottom: Scheme of the orbital epochs over which the spectra were averaged (Kijak et al. 2011).

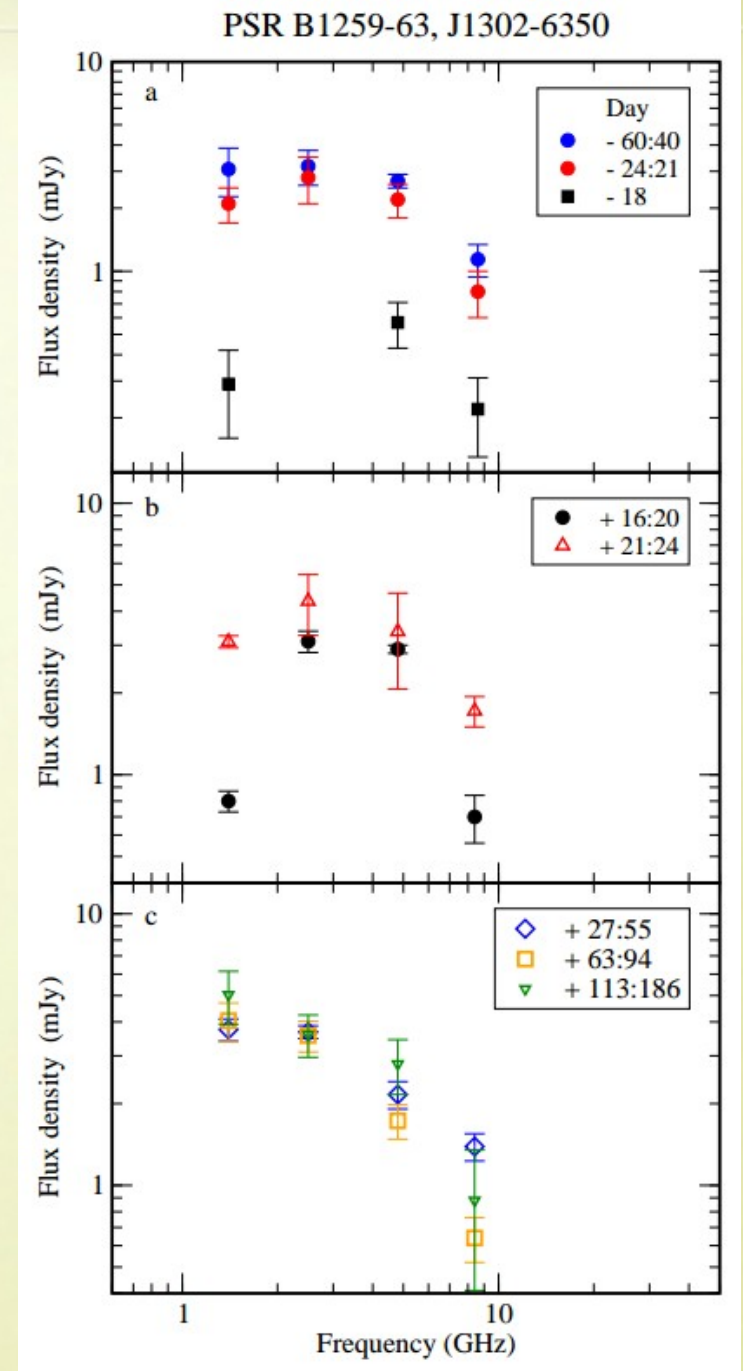


Figure 4: The spectra of PSR B1259-63 averaged over each orbital epoch (Kijak et al. 2011) 2/9

The observations of GPS pulsars

2021: 30 confirmed GPS pulsars

(18 associated with SNR, PWN, H II or EGRET/HESS source)

J. Kijak, W. Lewandowski,
O. Maron, Y. Gupta, A.
Jessner 2011 - introduced
the term gigahertz-peaked
spectra (GPS) pulsars as
analogy to GPS
extragalactic sources.

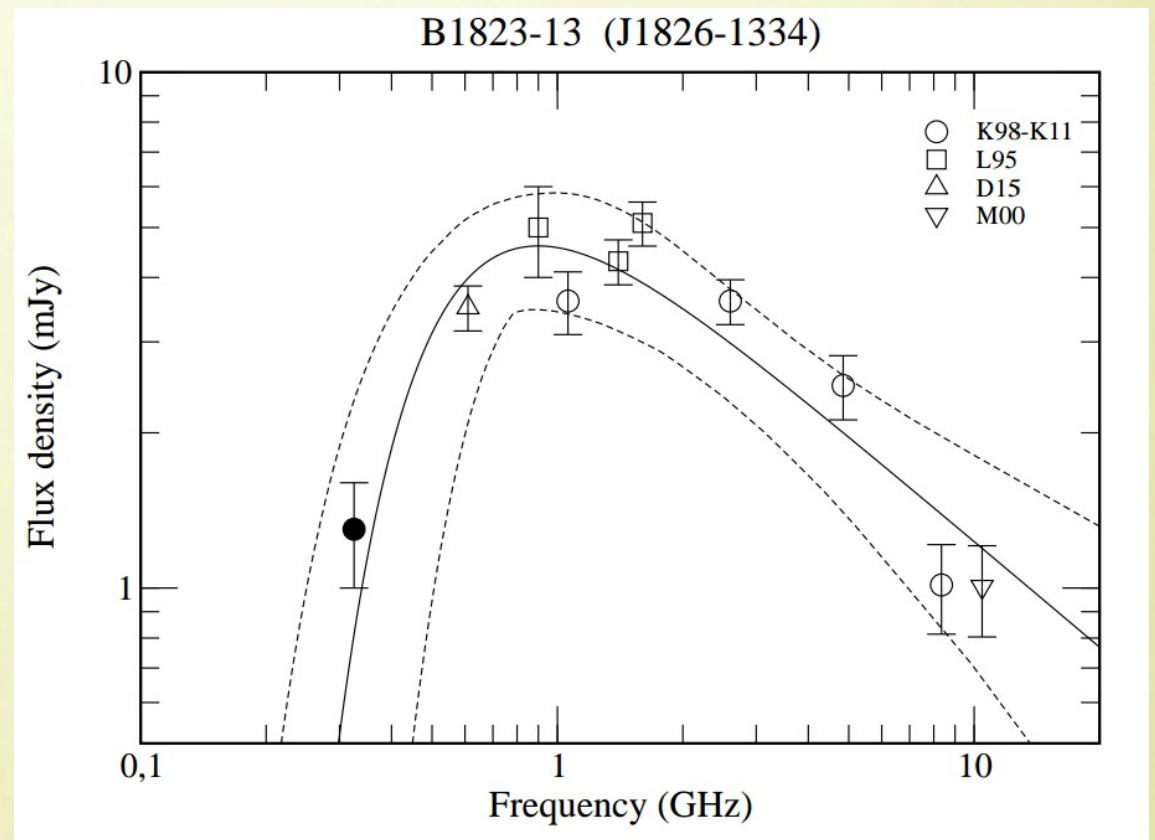


Figure 5: Example of GPS pulsar (Kijak et al. 2017a).

SGR J1745-2900 – SGR A* magnetar

1. The absorption in the electron material ejected during the magnetar outburst.

Our assumptions:

- The temperature drops adiabatically.
- Magnetar is located in the hot, dense environment.

2. An external absorption.

The thickness = 1 pc

$$n_e = 500 \text{ cm}^{-3}, T = 200 \text{ K}$$

Conclusion: the free-free thermal absorption model may explain the observed spectrum evolution.

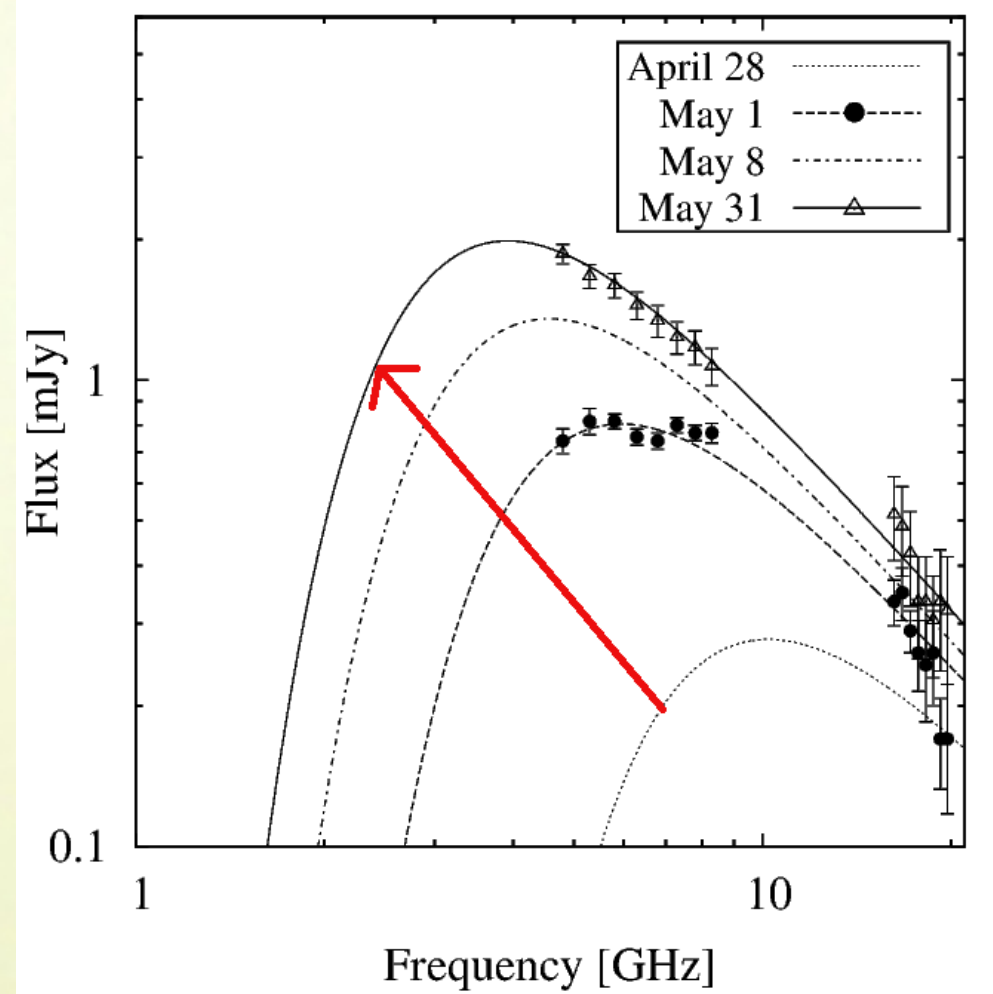


Figure 6: Spectra of the radio-magnetar SGR J1745-2900 with fitted free-free thermal absorption model. All values are taken from Figure 4 in Shannon & Johnston 2013. (Lewandowski, Rożko et al. 2015)

B1800-21 – Vela-like pulsar near W30 complex

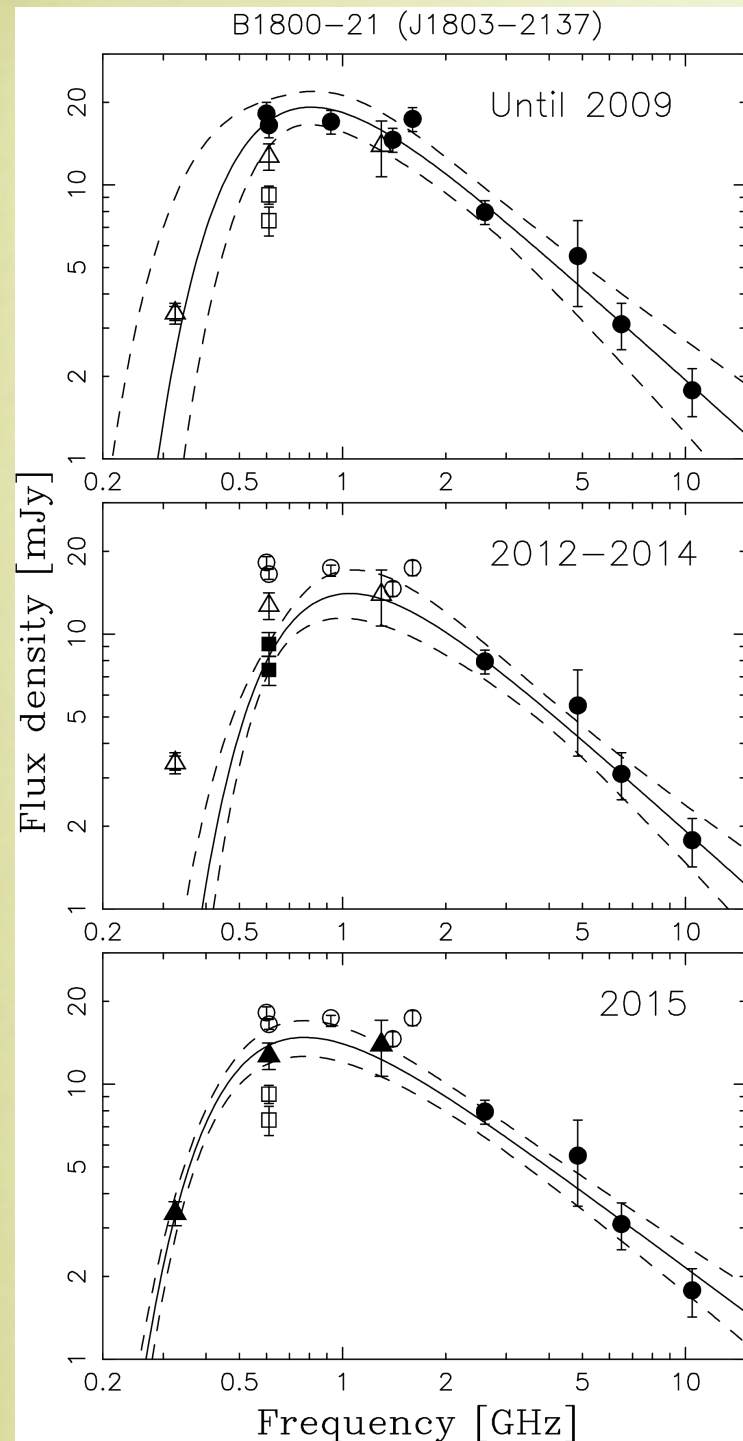


Figure 7: Basu, Rożko et al. 2016

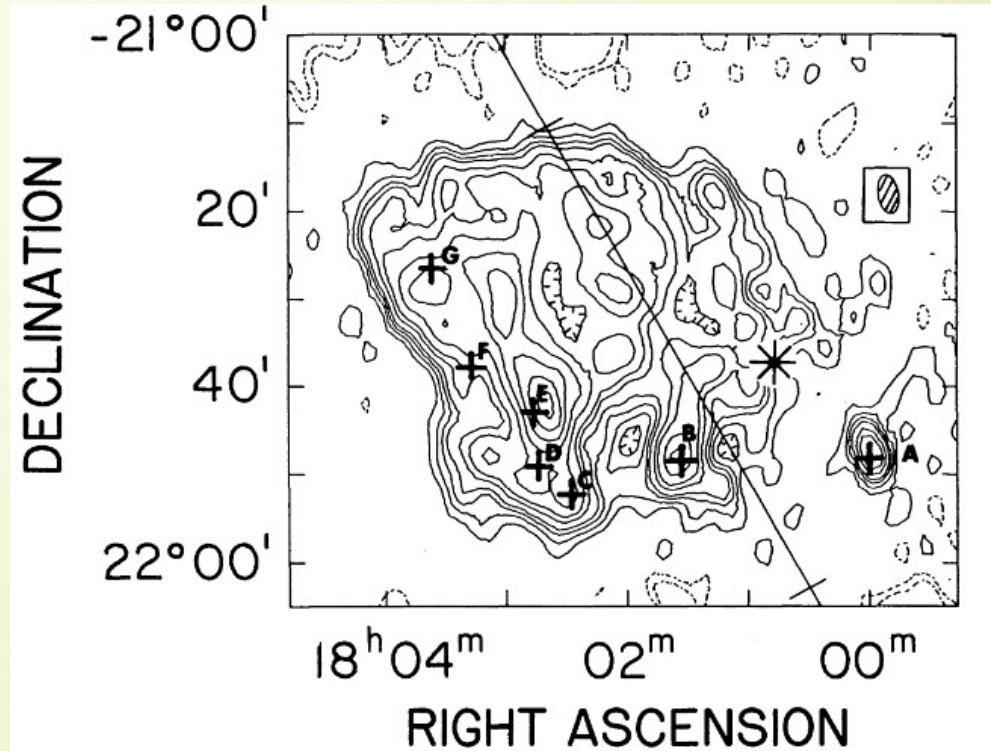


FIG. 1.—Contour map, corrected for primary beam attenuation, of the W30 complex at 90 cm wavelength (330 MHz). The half-power beamwidth of 4.1×2.8 at P.A. 11° is shown in the upper right-hand corner. Contour levels are at $(-0.50, -0.25, 0.25, 0.50, 0.75, 1.00, 1.50, 2.00, 3.00, \dots, 7.00) \times 0.5$ Jy beam $^{-1}$, with the peak brightness in the map being 3.76 Jy beam $^{-1}$ at the position $\alpha = 18^{\text{h}}02^{\text{m}}38^{\text{s}}$, $\delta = -21^\circ42'00''$. The brightness temperature scale is 1 Jy beam $^{-1} \approx 302$ K. The position of PSR 1800-21 is marked with a star (*), and the positions of known H II regions are marked with plus (+) signs and letter designations A-G. The Galactic plane is shown with tick marks at $l = 8^\circ$ and $l = 9^\circ$, with Galactic latitude increasing to the northeast.

Figure 8: Kassim & Weiler 1990.

J1740+1000 – the young pulsar far from the galactic plane

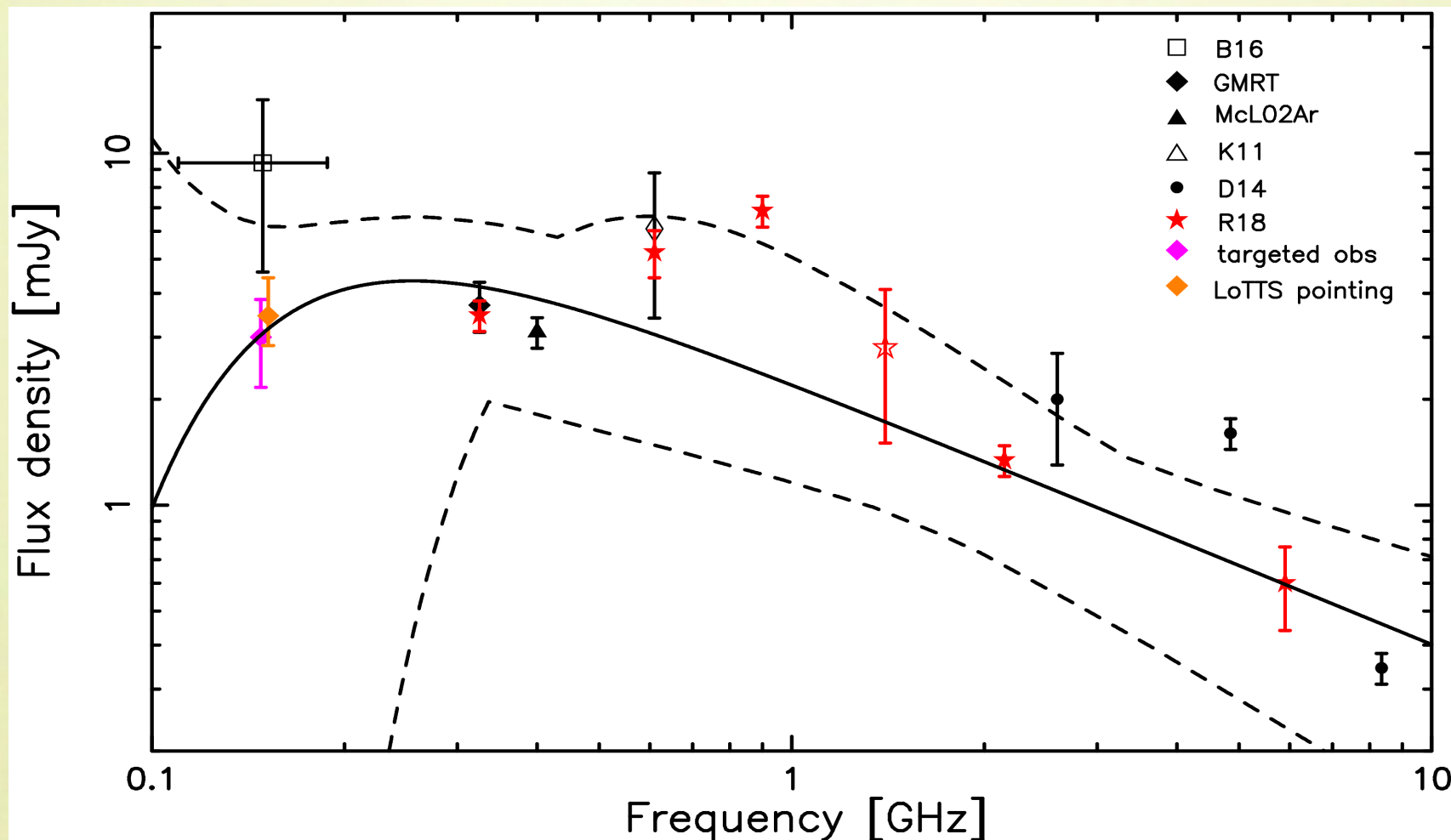


Figure 9: The pulsar spectrum with fitted free-free thermal absorption model based on all available flux density measurements.

The acronyms mean the following publications: B16 - Bilous et al. (2016), GMRT - our interferometry measurements published in Rożko et al. (2018), McL02Ar - McLaughlin et al. (2002), K11 - (Kijak et al. 2011b), D14 - Dembska et al. (2014), R18 - Rożko et al. (2018). (Figure from **Rożko** et al. 2020)

LOFAR observations of PSR J1740+1000

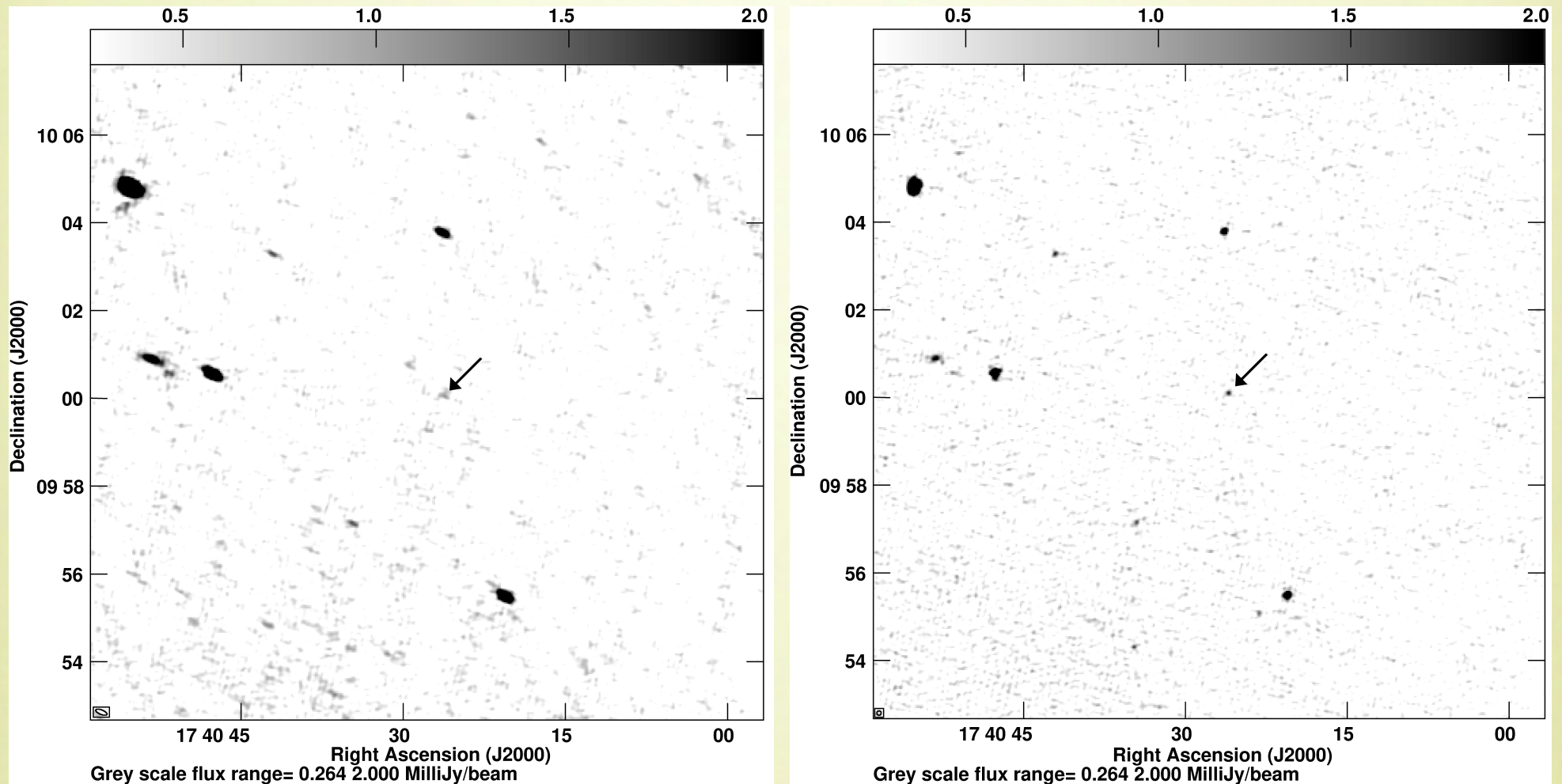


Figure 10: Grayscale images showing the total intensity maps centered at the region around PSR's J1740+1000 position (the black arrow marks the pulsar position). Both maps were obtained from the targeted observations. Left: results from the Factor pipeline. Right: results from DDF-pipeline. The map resolution is $16.5'' \times 6.2''$ and $6'' \times 6''$, respectively. (Figure from **Rožko** et al. 2020)

Wideband uGMRT observations of GPS candidates

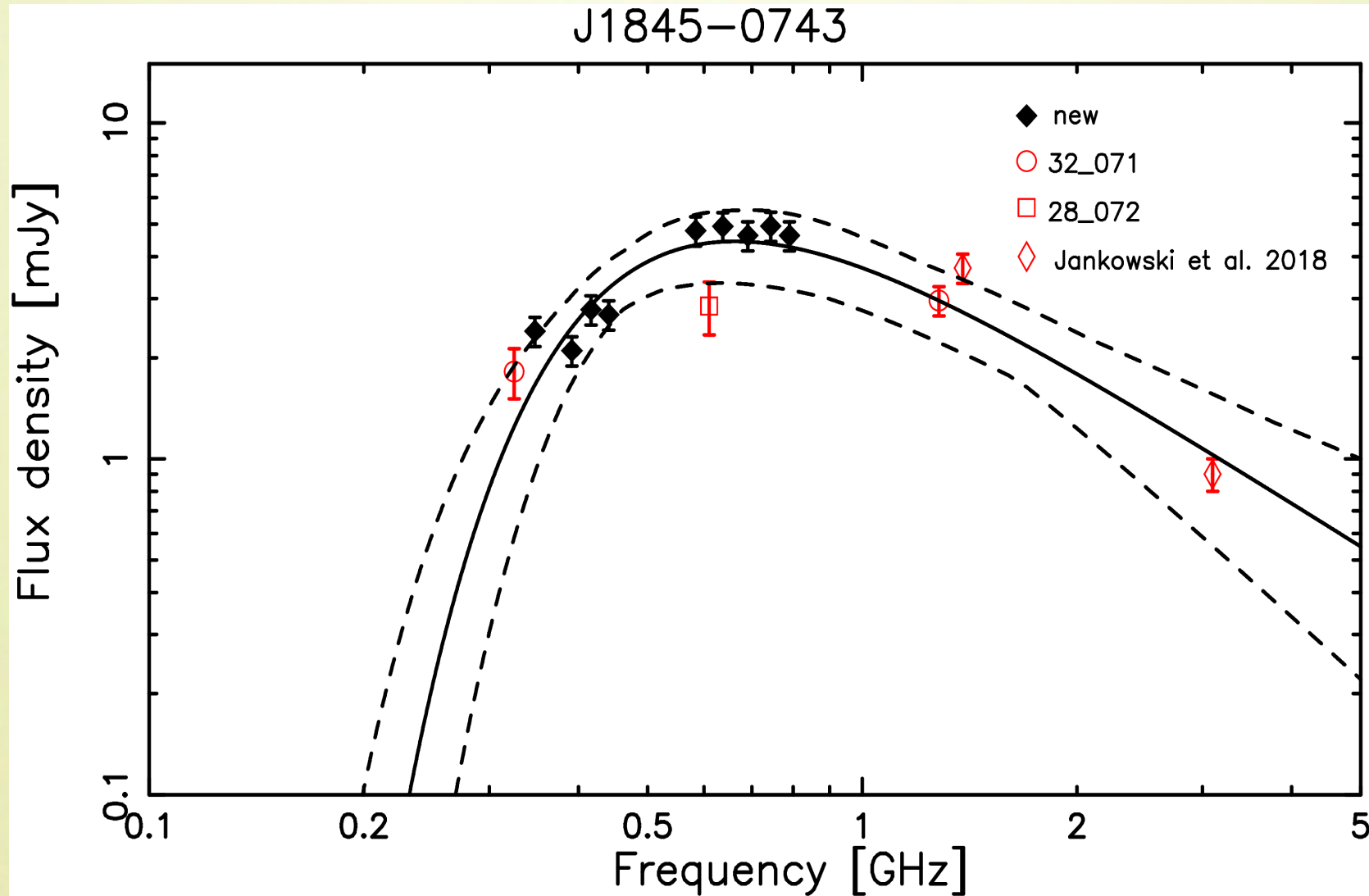


Figure 11: The PSR J1845-0743 spectrum with fitted free-free thermal absorption model. (Rożko et al. 2021, in preparation)

Future challenges

- Modelling of more complex spectral shapes:
- two absorbers along the line of sight?
- Or maybe we observed both: pulsar and pulsar wind nebulae emission?
- Comparison of the free-free thermal absorption model and synchrotron self-absorption model in cases when observed emission may come not only from pulsar but also from the Pulsar Wind Nebulae.
- Continuation with the wideband observations of the GPS candidates.

Thank you for your attention!

OUR MODEL:

$$I = Amp \times ((freq/10.)^\alpha) \times \exp(-1 \times freq^{-2.1} \times B)$$

FITTING PROCEDURE

The Levenberg-Marquard algorithm.

We fitted three parameters:

Amp - amplitude

α - spectral index

$$B = 8.235 \times 10^{-2} \left(\frac{T_e}{K} \right)^{-1.35} \frac{EM}{pc \text{ cm}^{-6}}$$

ERRORS ESTIMATION

3D χ^2 mapping: we calculate the matrix of χ^2 values for the fitted parameters and the values that are inside 1 sigma contour.

The constraints from DM

Table 5. Estimating the fitting parameters for the Gigahertz-peaked spectra using the thermal absorption model

| PSR | Amp | B | α | χ^2 | ν_p (GHz) |
|------------|---------------------------|------------------------|-------------------------|----------|------------------|
| J1740+1000 | $0.132^{+0.275}_{-0.094}$ | $0.22^{+0.11}_{-0.12}$ | $-1.61^{+0.66}_{-0.63}$ | 4.27 | 0.55 |
| B1800-21 | $1.65^{+1.52}_{-1.05}$ | $0.26^{+0.15}_{-0.10}$ | $-1.00^{+0.39}_{-0.49}$ | 8.94 | 0.76 |

From DM we can estimate n_e .

Using n_e we can calculate EM.

Using EM we can from parameter B calculate T_e .

And check if this has the physical sense.

$$B = 8.235 \times 10^{-2} \left(\frac{T_e}{K} \right)^{-1.35} \frac{EM}{\text{pc cm}^{-6}}$$

Table 6. The constraints on the physical parameters of the absorbing medium.

| PSR | Size (pc) | n_e (cm^{-3}) | EM (10^2 pc cm^{-6}) | T_e (K) |
|------------|--------------|-------------------------------|-------------------------------------|-----------------------|
| J1740+1000 | 0.1 | 119.48 ± 0.13 | 14.277 ± 0.030 | 106^{+42}_{-45} |
| | 1.0 | 11.948 ± 0.013 | 1.4277 ± 0.0030 | $19.3^{+7.6}_{-8.2}$ |
| | 10.0 | 1.1948 ± 0.0013 | 0.14277 ± 0.00030 | $3.5^{+1.4}_{-1.5}$ |
| B1800-21 | 0.1 | 1169.95 ± 0.25 | 1368.78 ± 0.58 | 2680^{+1100}_{-770} |
| | 1.0 | 116.995 ± 0.025 | 136.878 ± 0.058 | 488^{+199}_{-140} |
| | 10.0 | 11.6995 ± 0.0025 | 13.6878 ± 0.0058 | 89^{+36}_{-25} |

- The SNR filament:
size 0.1 pc
electron density 7000 cm⁻³
electron temperatur 5000 K
- The bow-shock PWN:
size 1.0 pc
electron density 50-250 cm⁻³
electron temperatur 1500 K
- The cold HII region
size 10.0 pc
electron density a few thousand cm⁻³
electron temperatur 1000-5000 K

Low-frequency turnover

Sieber (1973):

synchrotron self-absorption vs free-free thermal absorption

The case of PSR B0329+54

(K. Rajwade, D.R. Lorimer & L.D. Anderson 2015):

- the turn over frequency is around 200 MHz.
- the estimated EM is $\sim 0.052 \text{ cm}^{-6}$, for that value the fitted electron temperature is 0.18 K (which is contradicted to the assumed 5000 K - the typical temperature of the Warm Ionized Medium).

Conclusion: different mechanism may be responsible for the turnover at lower and higher frequency

Problem: thermal absorption could also cause turn over ~ 200 MHz, so it is hard to determine which model is correct one (it requires very good quality of pulsar spectrum)